



UNIVERSITÀ  
DEGLI STUDI  
FIRENZE

# FLORE

## Repository istituzionale dell'Università degli Studi di Firenze

### **Final design of the wavefront sensor unit for ARGOS, the LBT's LGS facility**

Questa è la Versione finale referata (Post print/Accepted manuscript) della seguente pubblicazione:

*Original Citation:*

Final design of the wavefront sensor unit for ARGOS, the LBT's LGS facility / Busoni, Lorenzo; Bonaglia, Marco; Esposito, Simone; Carbonaro, Luca; Rabien, Sebastian. - ELETTRONICO. - (2010), pp. 77365K-77365K-14. (Intervento presentato al convegno SPIE).

*Availability:*

This version is available at: 2158/609112 since:

*Terms of use:*

Open Access

La pubblicazione è resa disponibile sotto le norme e i termini della licenza di deposito, secondo quanto stabilito dalla Policy per l'accesso aperto dell'Università degli Studi di Firenze (<https://www.sba.unifi.it/upload/policy-oa-2016-1.pdf>)

*Publisher copyright claim:*

(Article begins on next page)

# Final design of the wavefront sensor unit for ARGOS, the LBT's LGS facility

Lorenzo Busoni<sup>\*a</sup>, Marco Bonaglia<sup>a</sup>, Simone Esposito<sup>a</sup>, Luca Carbonaro<sup>a</sup>, Sebastian Rabien<sup>b</sup>,

<sup>a</sup>Osservatorio Astrofisico di Arcetri, Lgo Fermi 5, 50125 Firenze (Italy);

<sup>b</sup>Max-Planck-Institut für extraterrestrische Physik (Germany),

## ABSTRACT

In this paper we present the final design of the WFS unit of LBT's ARGOS facility, that will implement a GLAO system using 3 Rayleigh pulsed beacons. The ARGOS WFS is composed of two main subunits: 1) a large dichroic window that deflects the laser beam toward the WFS and transmit the visible and near-infrared wavelength to the MOS-imager LUCIFER and 2) the SH-WFS that collects the backscattered light of the 3 beacons and combines the beams on a single lenslet array and detector. The WFS unit includes Pockels cells for the range gating of the laser beams, field and pupil stabilizers to compensate for the fast jitter of the laser beams and for optical flexures and a calibration unit to check the internal alignment; this unit will be also used for closed-loop laboratory tests using a MEMS-DM.

**Keywords:** Laser Guide Stars, Large Binocular Telescope, Wavefront Sensor, Pockels cells

## 1. INTRODUCTION

ARGOS is the Laser Guide Star facility of the LBT implementing a Ground Layer Adaptive Optics system [6] capable of enhancing the image quality for the multi-object spectrographs and NIR imagers LUCIFER over a wide field of view under almost all seeing conditions [1].

The system makes use of three 18W green lasers for each LBT's eye to produce 3 beacons at 12km. The backscattered light is split from the scientific wavelengths by a large dichroic window tilted in front of the AGW unit (containing the guider and the NGS pyramid wavefront sensor) and LUCIFER. The window shape has been designed with a cylindrical surface to compensate the aberrations induced on the instrument focal plane and the coating design minimizes the thermal impact onto the instrument. The dichroic beam splitter optical and mechanical design is described in Section 2.

The deflected light is collected by a Shack Hartmann wavefront sensor whose optical design is conceived to image the 3 spot patterns on a single large, fast and low-noise CCD described in [2]. On each WFS beam, a motorized field lens will finely adjust the position of the pupil images on the lenslet array and a tip-tilt piezo mirror pupil-conjugated will stabilize the Shack-Hartmann spots within their subapertures. Details of the optical design and of the simulated performances of the WFS are given in Section 3.

Acquisition cameras patrol the Rayleigh beacon focal plane over a 1 arcmin FoV to assist the acquisition process in case of mechanical flexures after telescope slewing. In case of deflection of the beam out of the WFS entrance field stop (5 arcsec FoV), the patrol camera will send corrections to the launch system [5] to adjust the on sky laser pointing and track the beacon back to the WFS field. Patrol cameras are described in Section 4. A calibration unit described in Section 5 will be used to check for internal alignment of the WFS and for closed-loop functionality tests using a MEMS deformable mirror.

The straylight light is sliced by Pockels cell to gate out the desired backscattering range. A novel concept of Pockel cell with revised materials and optical setup improving the transmission performances has been developed and is described in Section 6.

## 2. DICHROIC BEAM SPLITTER

The laser light backscattered from the atmosphere is deflected toward the WFS by a large dichroic plate placed before LUCIFER. The dichroic coating has to transmit the scientific light (600-2450nm) and to reflect the shorter wavelengths,

\*lbusoni@arcetri.astro.it; phone +39 055 2752 202

being optimized for maximum reflectivity at 532nm (Rayleigh LGS) and 589nm (sodium LGS, for future ARGOS upgrade [3], [4]). The coating on both surfaces is required to have a small reflectivity in K band to avoid injection of thermal dome background into LUCIFER.

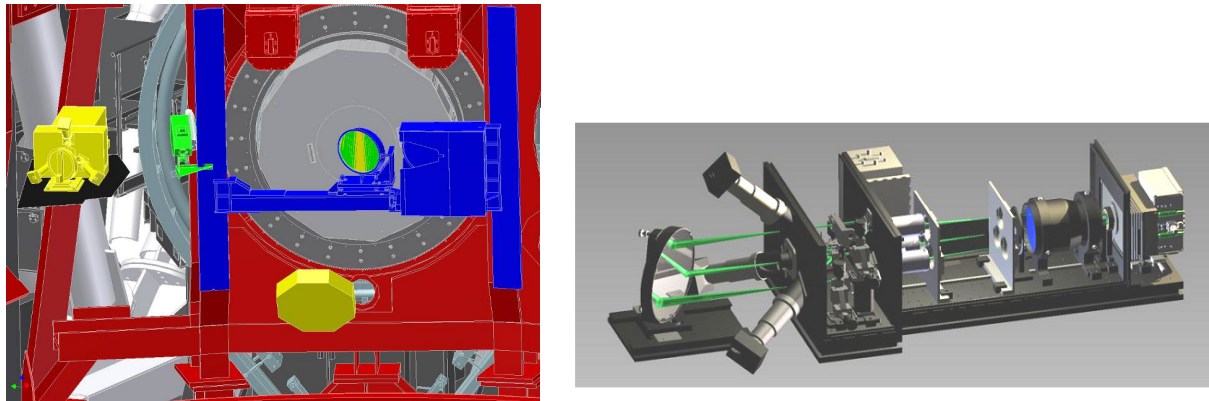


Figure 1 (left) Global view of the ARGOS WFS system. The dichroic unit is shown in blu, the yellow box on the black table represents the LGS WFS. The small green box is a possible implementation of the foreseen WFS for the on-axis sodium beacon [3], [4]. The supporting structures of the LGS WFS and of the tertiary mirror are not shown in this figure. (right) view into the mechanical arrangement of the WFS setup.

The plate's shape is designed to compensate the aberrations introduced on the transmitted beam by the thick, tilted window. The beam quality on LUCIFER (after proper alignment of the hexapod and the application of a small static coma on the ASM) is practically unaffected by the presence of the dichroic plate. The thickness of the plate as well as the mounting frame have been designed in such a way that the displacement and the bending of the plate when the telescope elevation is changed are negligible. The window can be moved to the working position when ARGOS is used and then slide out to a parking position that leaves totally unobstructed the optical path in front of the AGW unit.

The entire assembly is bolted to the rotator structure in front of the AGW in a volume shaped in such a way to avoid vignetting of the primary mirror and to permit the deployment of LUCIFER calibration unit when the dichroic is in its parking position.

## 2.1 Optical design

The dichroic window is tilted of  $40.5^\circ$  with respect to Lucifer optical axis, it has a size of 300x400mm, a clear aperture of 290 x 390mm and a thickness of 40mm. The glass is INFRASIL 302, that has minimal absorption in K band.

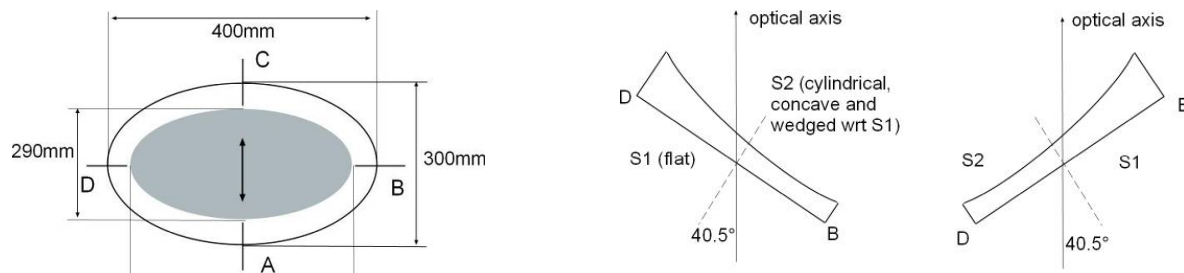


Figure 2 Geometry of the optical component to be manufactured (drawing not in scale). The gray surface corresponds to the optical area, the 10mm blank edge is needed by the mount system. The double arrow in centre shows the direction of polarization of the laser. On the right, horizontal cut of the optical windows (sx and dx telescope, drawing not in scale).

The front surface is flat; to compensate the aberrations introduced by the thick, tilted window, the second surface (the one facing the AGW unit) is cylindrical ( $R=230\pm 20\text{m}$ ) with the cylinder axis oriented along the ellipse minor axis and wedged ( $0.56\pm 0.02^\circ$ ) with respect to the first surface with the wedge along the ellipse major axis (Figure 2).

## 2.2 Image quality on Lucifer and on AGW

The optical quality of the pure telescope on Lucifer focal plane, in absence of the dichroic are summarized in Figure 3.

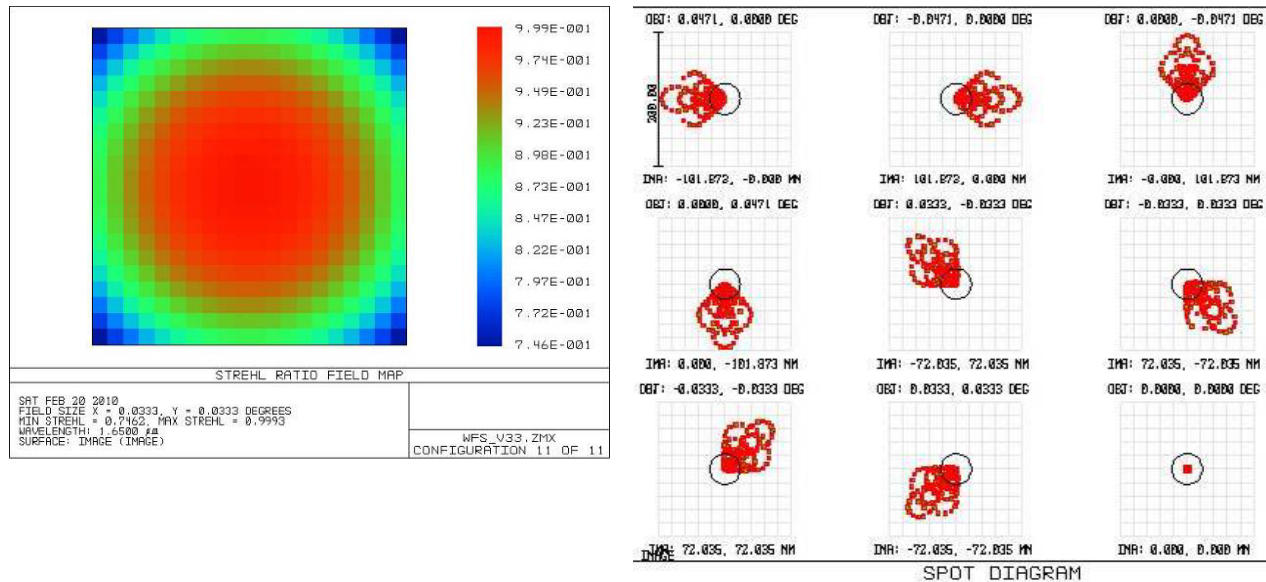


Figure 3 Optical performance of the pure LBT telescope. No dichroic is considered. Spot pattern and SR as a function of FoV position. Maximum distance is  $2\sqrt{2}$  arcmin to probe the square  $4\times 4$  arcminutes FoV of LUCIFER.

When the dichroic is placed into the optical path, the alignment and the static shape of the Adaptive Secondary Mirror (ASM) have to be modified to obtain the best optical quality on LUCIFER focal plane. The ASM is decentered of  $-0.35$  mm along the y axis and tilted of  $-0.0195^\circ$  around the x axis;  $342\text{nm}$  of astigmatism Z6 are applied to the ASM. Focus is corrected by z-shifting the hexapod of  $68\mu\text{m}$ . The optical quality after this collimation process is shown in Figure 4 demonstrating that the aberrations induced by the presence of the thick dichroic window in the scientific path can be perfectly compensated.

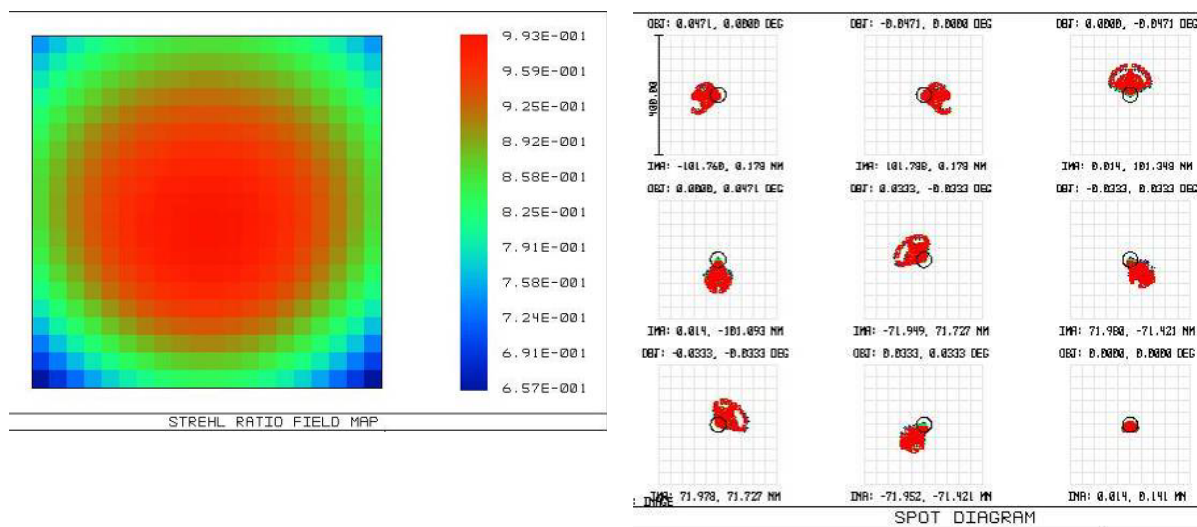


Figure 4 Optical performance of the LBT telescope when ARGOS dichroic is in its working position and ASM alignment and shape have been optimized. Spot pattern and SR as a function of FoV position. No significant difference in optical quality over the entire LUCIFER 4x4 arcmin field of view with respect to the “pure telescope” case of Figure 3.

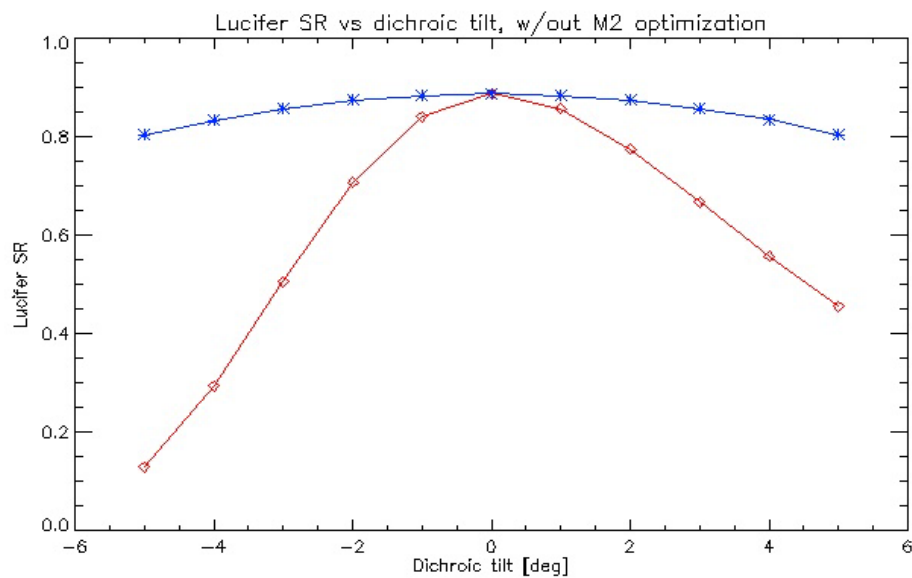


Figure 5 Average SR on LUCIFER FoV when the dichroic is tilted with respect to its nominal position ( $40.5^\circ$ ) around major axis (top curve) and minor axis (bottom curve). No optimization is done on the ASM that is kept in the same shape that maximize the SR when the dichroic is in the nominal

In Figure 5 the LUCIFER Strehl ratio averaged over the 4x4' FoV is shown as a function of the tilt angle around the axes of the dichroic window. The tolerance for the rotation around the major axis is quite large, in the order of  $\pm 4^\circ$ ; tighter tolerance is needed for the rotation around the minor axis where  $\pm 1^\circ$  is acceptable with a mean loss of SR of 5% over the entire FoV.

On the WFS optical path the tolerances on the dichroic positioning are tighter. The reflected beams must stay in the patrol camera FoV for the system to be capable of measuring the position of the laser spots and repoint the laser on sky in order to hit the WFS entrance window. This condition turns into an allowed positioning error for the dichroic of  $0.2^\circ$  in both tilt and tip and 10mm of piston of the window (not cumulated with rotation around the minor axis).

The bottom line of this tolerance analysis is that the quality of LUCIFER image is not critically dependent on the dichroic positioning. During the installation, after having aligned and optimized the ASM to get the best image on LUCIFER, one still has the possibility to rotate the dichroic around its major and minor axis of up to  $4^\circ$  and  $1^\circ$  respectively to center the beams on the WFS. Once everything is aligned, the repeatability error in the positioning of the dichroic window, as well as the dichroic tilt induced by flexures in the mechanical structures, has to be less than  $0.2^\circ$ .

### 2.3 Coating

The thermal analysis conducted for PDR shows that a total reflectivity of 2% in K band for the dichroic coating contributes negligibly to the thermal background (Figure 6).

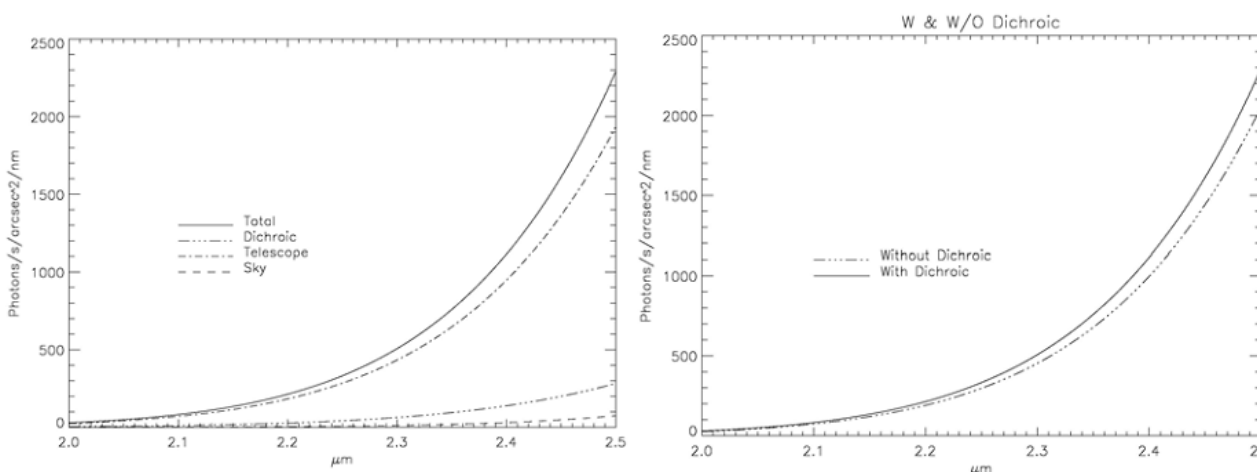


Figure 6 Thermal background photons from a blackbody model arriving in the LUCIFER focal plane. The background is assembled from the warm sky, telescope, and the dichroic contributions. The by far largest amount of thermal background is contributed by the warm aluminium surfaces of the telescope. We assumed: sky temperature 220K, telescope temperature 273K,  $R_{\text{telescope}} = 0.95^3 = 0.86$  (3 aluminium mirrors),  $R_{\text{dichroic}} 0.02$  (K band spec of the combined coatings)

The dichroic has been identified as a critical component for the ARGOS project mostly because of the uncertainties about the feasibility, achievable quality and durability of the coating in a harsh environment. To mitigate the risk, witness samples will be produced and tested under stress conditions before coating the final units. A calculated transmissivity profiles from Layertec GmbH matching the required specifications is shown in Figure 7.

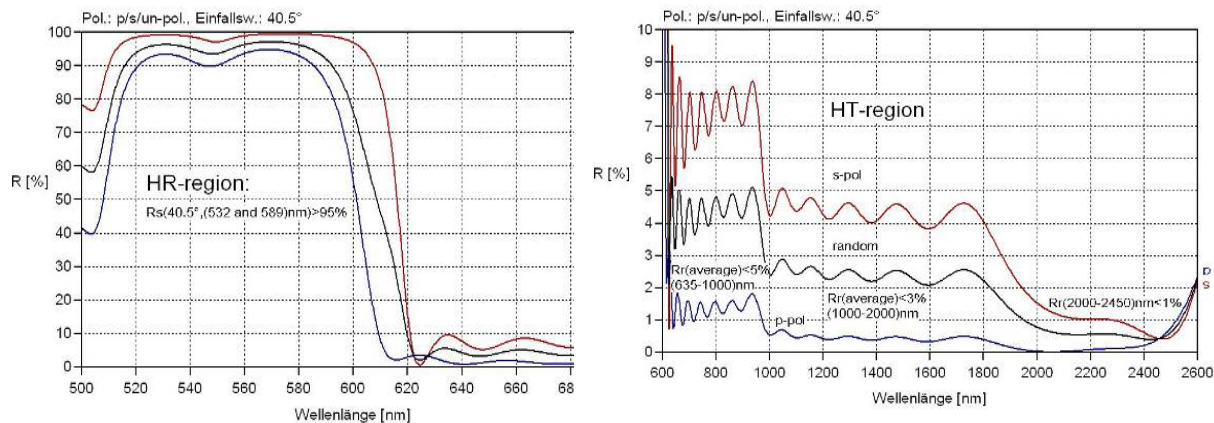


Figure 7 Computation of coating performances from Layertec GmbH. Left: high reflectivity region, optimized to reflect 532 and 589nm. Wavelength above 620nm are transmitted. Right: transmission in the scientific wavelength range. In K band the reflectivity is <1% for each surface, matching goal specifications.

## 2.4 Mechanical Design

The Argos calibration system supports the dichroic mirror and provides the possibility of moving it along a railway to free the field of view. The system has also a simple mechanism that permits to correct the height of the mirror, its piston along the main optical axes and its tip and tilt (Figure 8).

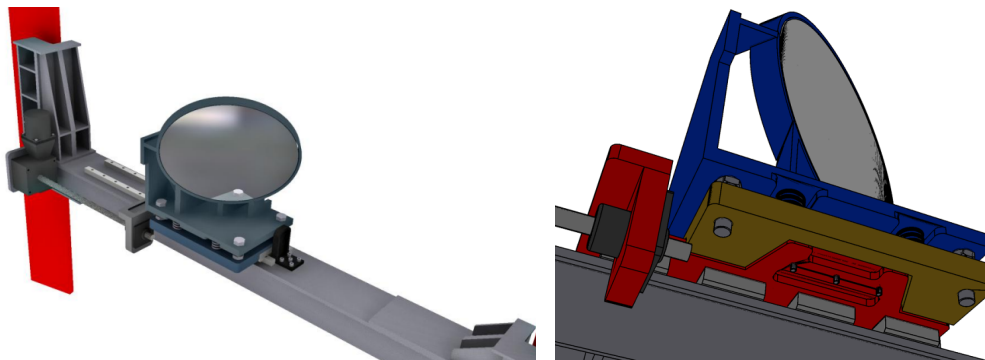


Figure 8 View of the dichroic support and mount to the telescope, without the “garage” box. Centering system of the dichroic. The red frame is always fixed to the carriages, during the alignment the yellow one can slide on it, while the blue frame lays over four springs. The preload on these springs can be changed by the big vertical bolts in the figure, changing the height of the mirror and eventually its tilt angle around the horizontal axis passing by its center



The total estimated mass of the unit, window included, is 250Kg. A finite elements analysis have been performed to check mechanical stability of the dichroic under the effects of gravity. The model has been developed using only shell and beam elements. The results refer to a coordinate system where the X axes is the same of the optical axes of Lucifer and the Z axes is parallel to the telescope optical one. The center of the coordinate system is located in the center of the dichroic.

Table 1 resumes the most interesting results for what concerns the mechanical stability of the mirror; note that the values of displacements and rotations reported are the highest detected over the mirror surface. The first Eigen mode of the structure is at 47 Hz. The computed deflections are well inside the acceptable ranges.

LOAD CASE	Maximum dichroic tilt (deg)	Maximum dichroic displacement along X (microns)	Maximum dichroic displacement along Y (microns)	Maximum dichroic displacement along Z (microns)
Gravity: 1G along Z (telescope at Zenith)	<b>0.0053</b>	<b>44.1</b>	<b>Less than 10</b>	<b>59.7</b>
Gravity: 1Gcos15 along Y +1Gsin15 along X (telescope at the horizon)	<b>0.0084</b>	<b>62.1</b>	<b>86</b>	<b>Less than 10</b>

Table 1 FEA results. Tilt and displacement of the window under the effect of the gravity are well inside the acceptable range.

### 3. RAYLEIGH BEACONS WFS

The main requirements for the ARGOS WFS are listed below:

- Sense the wavefront of the 3 ARGOS LGS arranged on a triangular asterism of 2 arcmin radius with 3 SH WFS having 15 subapertures and 5 arcsec FoV.
- Arrange the 3 SH patterns on a single 256x248 pixel detector with 48μm pixel-size. The detector is described in [2].
- Host gating units to gate the range of altitudes from which the backscattered light can reach the sensor. (see Section 6 for a description of the Pockels cells).
- The WFS must be provided with 3 large field cameras (1 arcmin FoV) to track the laser spots on sky and to control the laser pointing system in closed-loop. These elements are described in Section 4.
- The WFS must provide field stabilization devices to compensate for the jitter of the laser spots on sky.
- The WFS gating units must be fed with 3 collimated beams of 6mm diameter. The beams are maintained parallel to the WFS mechanical axis by the field stabilizers.
- The WFS is fed with monochromatic light at 532 nm.
- To compensate any mechanical flexures that can affect the position of the pupil, the system must implement a control loop that estimates the position of the pupils from the CCD frame and adjust the position of the beams on the lenslet array independently for each one of the 3 beams.
- An internal calibration unit is needed to check the WFS alignment in laboratory and at the telescope. This device can be provided with a deformable mirror that will be used during the closed-loop tests in laboratory.
- A shutter and a flat field illuminator are needed to calibrate the WFS detector.
- Because of the high number of optical elements that compose the WFS system their transmission or reflection coefficient at 532nm must be as high as possible; V-coating ( $R < 0.25\%$ ) is used whenever possible.



- Maximum care must be taken to reduce aging of the coatings and dust contamination. The WFS enclosure will be sealed and it will be flushed with a slight overpressure of dry air to keep the dust out of it. Critical optics, as the WFS entrance windows or the detector window, will be continuously flushed with dry air.

### 3.1 Optical Design

The optical layout of the WFS is shown in Figure 9. For the sake of simplicity, only one of the 3 beams is shown. The LGS beam reflected by the fold mirror (on the left) is focused on the WFS entrance window that acts as field stop for the WFS: a 4.7 arcsec FoV around the nominal laser beacon position is transmitted to the SH WFS, while off-axis sources are reflected toward an acquisition camera, patrolling a 60" FoV. The back side is used as reflecting surface, to feed the light from the internal calibration unit toward the SH WFS (see Figure 10).

The 3 beams have independent optical paths up to the final collimator that arranges the 3 SH patterns on a single lenslet array and on a single detector.

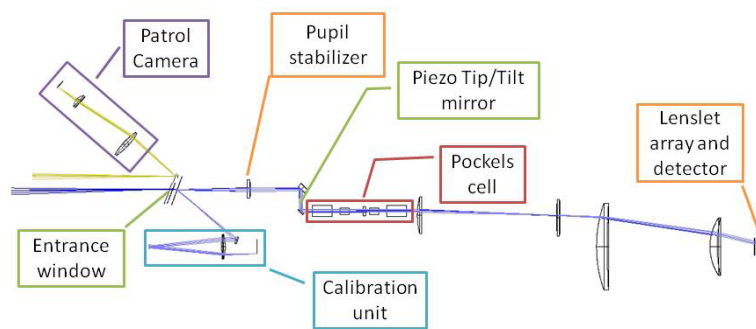


Figure 9 Optical design layout of the SH WFS.

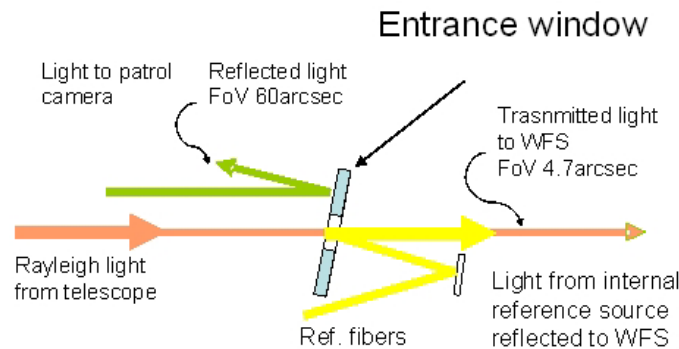


Figure 10 Sketch of the various reflections on the entrance window of the ARGOS WFS.

The elements that compose a single arm of the sensor are listed below, from left to right in Figure 9:

- The entrance window that acts as field stop for the SH WFS.
- A collimating lens that provides a collimated beam for the gating units and steers the 2' off-axis beam in to make it parallel to the WFS mechanical axis. This lens can be remotely displaced in the XY plane to adjust the pupil image position on the lenslet array.
- A periscope assembly, composed by a folding mirror and a piezo-driven mirror. This device is used to reduce the distance between the 3 beams axis and reduce the size of the final SH collimator. The Physik Instrumente S-334.2SL piezo mirror is conjugated to the telescope pupil and it is used to compensate the LGS beam jitter. The mirror is V-coated with high reflectance (>99%) at 532nm optimized for an angle of incidence of 45°.
- A Pockel cell unit to select the scattering height range.

- A refocusing lens and a field lens are used to match the pupil position on the lenslet array and the SH spot grid on the detector pixel grid. Because the CCD read-out is split in two rectangular areas of 128x248 pixels, the first arm pupil is decentered of 4 pixels so that no 8-by-8 pixel group related to a single subaperture is split onto the 2 semi-frames.
- A single SH collimator made of 2 custom lenses.
- A single lenslet array refocuses the 3 collimated beams on the detector. Lenslets have square geometry, with a lens pitch of 384 $\mu$ m, and a RoC of 6.15mm. The array contains 62x62 lenslets and has a size of 24mm and a thickness of 1.2mm.
- The 3 SH spot patterns are arranged on a single CCD as shown in Figure 11.

The 3 beams have a 120deg rotational symmetry around the WFS mechanical axis. The symmetry is broken by the fact that the triangular symmetry of the beams on sky cannot be matched on the square geometry of the lenslet array and of the detector: as a consequence of that, the refocusing lenses and field lenses are decentered with respect to the optical axis in order to center both pupil and spot pattern on the proper position on lenslet array and detector respectively.

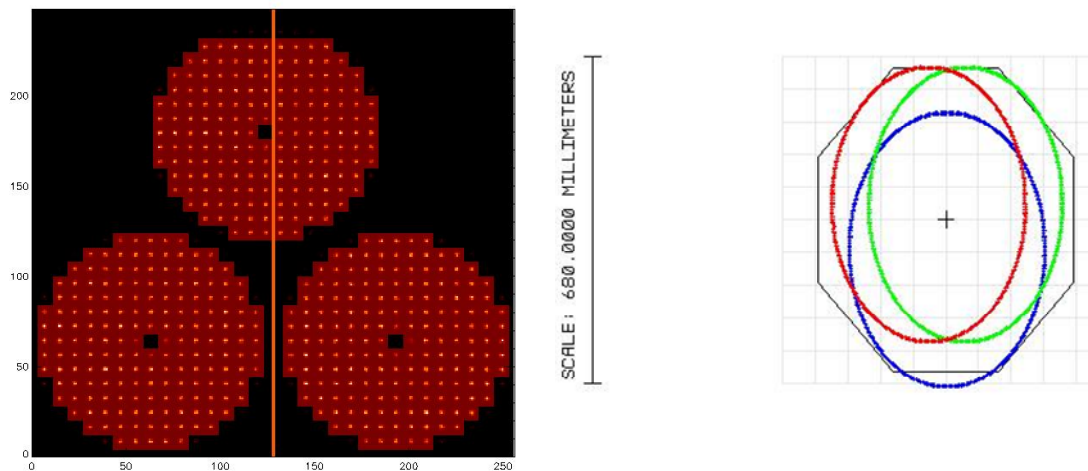


Figure 11. Left: Simulated CCD frame obtained from Zemax considering a reference source of 1" FWHM at 12 km altitude. The 3 red areas correspond to the 15x15 subaperture patterns on the CCD. The orange vertical line marks the separation of the two halves of the CCD and makes evident the 4 pixels decenter of LGS1 spot pattern. Right: Footprint on M3 of the LGS beacons, showing the vignetting of the top row of subapertures of LGS1 (blue in the figure)

The main characteristics of the Shack-Hartmann sensor are summarized in Table 2.

Table 2 Main optical parameters of the SH WFS

Specification	Reference value
Number of subapertures on pupil diameter	15
Lenslet pitch	0.384 $\mu$ m
Number of pixels on subaperture diameter	8
Lenslet array radius of curvature	6.15 mm
Focal plane scale	85 $\mu$ m/arcsec

Pixel scale	0.56 arcsec/pix
Lenslet FoV	4.6 arcsec
Spot geometrical radius	10 $\mu\text{m}$ / 0.12 arcsec
Lenslet diffraction limit	22.7 $\mu\text{m}$ or 0.27 arcsec
Pupil ellipticity on lenslet due to incidence angle	1% (incidence angle 0.16 rad)

#### 4. PATROL CAMERAS

The 3 patrol cameras will be used to find the reference laser spot in a FoV of 60 arcsec diameter. The cameras receive the light after reflection on the coated area of the WFS entrance windows (diameter 40.5mm) that are located close to the Rayleigh LGS focal plane. The patrol cameras have a plate scale of 250  $\mu\text{m}$  per arcsec. A FoV of 60 arcsec diameter fits into a 15 mm square size CCD. The patrol cameras are DVC-4000AM, having a 2048x2048 detector with square pixels of 7.4  $\mu\text{m}$  (30mas). A binning by 4 is sufficient from a resolution point of view.

The patrol camera are placed before the gating unit of the WFS, therefore they integrate the Rayleigh light backscattered from the entire atmosphere. Laser backscattered flux from the gated range (11850-12150m) is expected to be 1800 photons / subaperture / ms [1] which translates to 300 Mph/s over the entire telescope pupil. An analysis of the spreading of the photons over the patrol camera field (see Figure 12) shows that, in spite of the patrol camera being not gated, only the light backscattered from a 1000m range around 12 km height is properly focused and mostly contributes to the estimation of the laser pointing position. With a spot size of 1 arcsec, the number of binned pixels receiving 90% of the flux is around 300, meaning an average of  $1\text{e}6$  e-/px/s. An exposure time of 0.03s or less should provide a good signal without reaching the saturation of the sensor (35000ph).

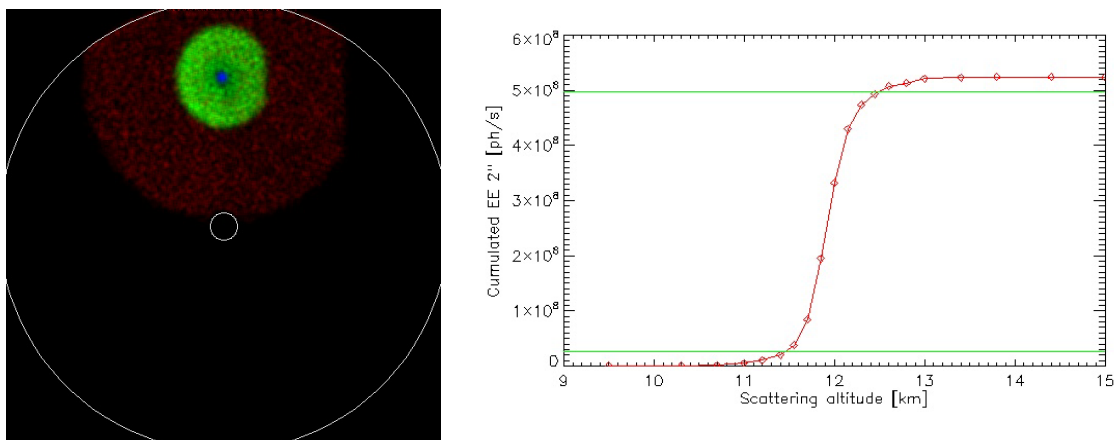


Figure 12 Left: Patrol camera images of light backscattered from different altitudes (red = 9.5km, green = 11km, blue = 12km). Intensities are not in scale. The 2 circles define the annular patrol camera FoV. Right: Flux in a 2x2 arcsec square around the peak. 90% of the intensity of peak comes from between 11.5 km and 12.5 km. Intensities are scaled to correspond to the nominal return flux (1800ph/ms/subaperture integrated from 11.85 to 12.15km)

## 5. INTERNAL CALIBRATION UNIT

This device has been designed for two main purposes: 1) to allow a fast check of the internal alignment of the WFS and 2) to provide the optical setup needed to test the WFS in closed loop in the laboratory.

The optical design of the WFS calibration unit is shown in Figure 13.

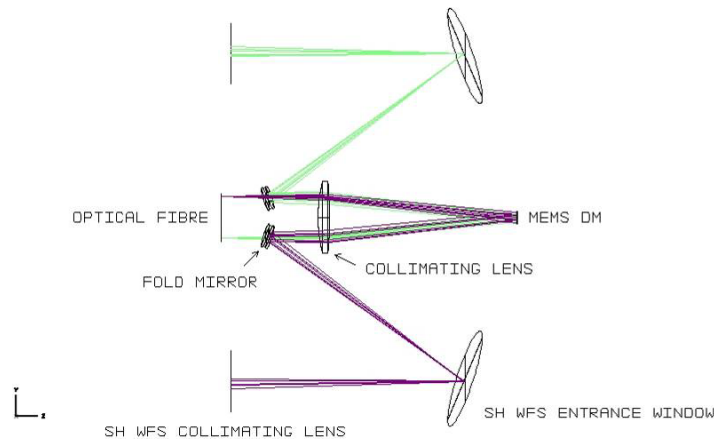


Figure 13. Optical design of the internal calibration unit of the ARGOS WFS.

A 600  $\mu\text{m}$  optical fiber placed 10mm off-axis creates a source simulating an 0.85 arcsec on-sky spot on the SH WFS; a double pass lens collimates the beam coming from the fiber and refocuses the beam reflected by the pupil mirror. A mirror with superimposed a circular stop of 4.8 mm acts as pupil. This mirror will be a commercial flat mirror during the first alignment of the WFS and once it will be installed at the telescope. During the WFS test in laboratory, this mirror will be replaced by a MEMS-DM to perform closed-loop tests. The beam reflected by the mirror is focused by the double-pass lens and deflected on the back of the entrance window. After that, the beam follow the path toward the WFS detector with the same f-number, focus and direction of the beam incoming from the on-sky beacon.

The deformable mirror for the closed-loop test is a MEMS (Boston MULTI-DM) with 12x12 actuators having a 4.9 mm side. It is controllable via an USB port and it is capable of a frame rate  $> 1$  kHz.

A circular stop of 4.8mm diameter must be placed in front of the MEMS-DM to reproduce a circular pupil. Because the 3 calibration unit beams have a wide angle of incidence of  $6^\circ$ , the stop must be placed within 0.1mm from the DM surface to ensure that the actuator pattern seen by the 3 beams is shifted by a negligible amount (less than 1/10 of subaperture). To place the stop so close to the DM surface a customized DM enclosure has been designed.

## 6. POCKELS CELLS

For gating out the desired slice of straylight ARGOS uses Pockels cells in the beam train of the wfs. A wide review of possible materials and designs has been done during preliminary design. The outcome is a novel Pockels cell setup developed at MPE that fulfills all requirements.

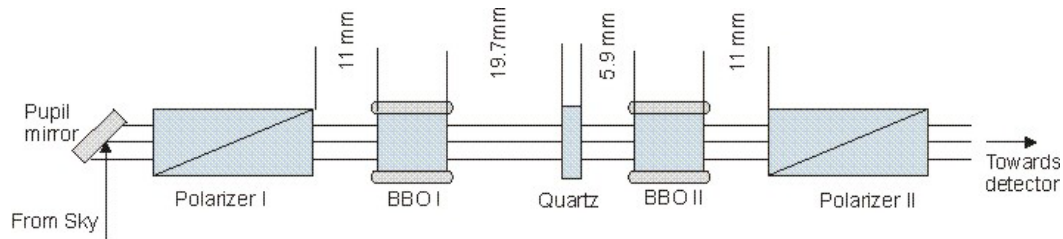


Figure 14: scheme of the Pockels cell optical setup. Between two polarizers the electrooptical crystals are placed. The distances that came out of the mecha

The Pockels cell principal is shown in Figure 14. It consists of the electrooptical crystals that are placed between two polarizers. The design of the cell is optimized for highest transmission, best suppression rate and clean, ringing free switching behaviour.

All 3 pockels cells will be controlled by one driver, fixed to the WFS enclosure to reduce the length of HV cables. The HV power supply and the delay generator will be located in the WFS electronic cabinet. To avoid EMC problems due to the fast hv-switching, the cells and the cables inside the WFS enclosure will be capsuled in a separate EMC housing. The high voltage switching circuit follows a bipolar push-pull scheme. The main requirements are summarized:

- capacitive load (3x 2 BBO crystals, each 10x10x12mm)
- Rise- and Fall time <20ns, output pulse jitter <2ns
- On-time 300ns...4 us
- Repetition rate 9-12kHz, typ. 10kHz

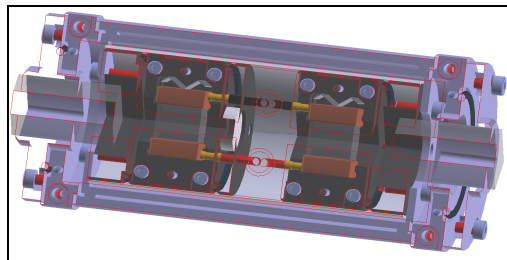


Figure 15 View into the pockels cell unit. From left to right the clean up polarizer is followed by the first BBO then the quartz rotator and the second BBO and finally the polarizer II.

## 6.1 Pockels cell performances

In a test setup at MPE the principle and the performance of the cell has been measured with sending a converging light beam through the cell and imaging the transmission in on and off state.

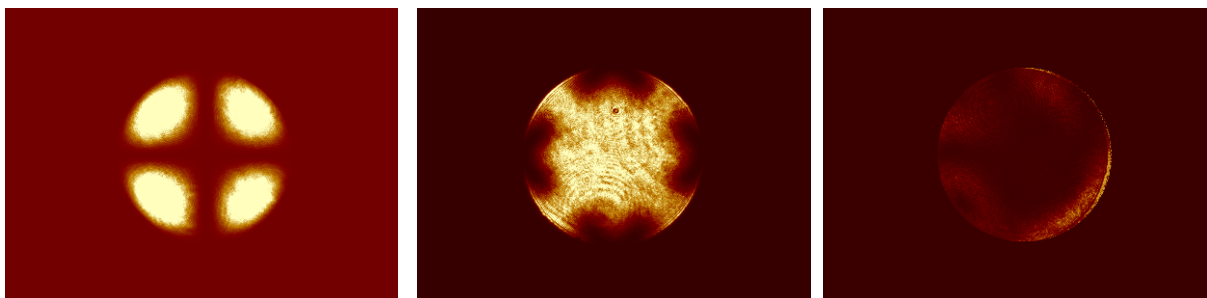


Figure 16: convergent light transmission through the Pockels cell setup. To the left the transmission through a 12mm thick BBO is shown for comparison. In the center the field dependent transmission in the on-state is shown. The right image shows the transmission when the cell is in the off-state. The intensity scale is not the same for the images.

Figure 16 shows some images of the convergent light transmission. When using a 'normal' pockels cell, the birefringent properties cause the known 'cloverleave' image. Practically this means that the usable field of view is very small. With the developed compensated cell the suppression stays high over a larger field, and even in the center can be better than a normal cell.

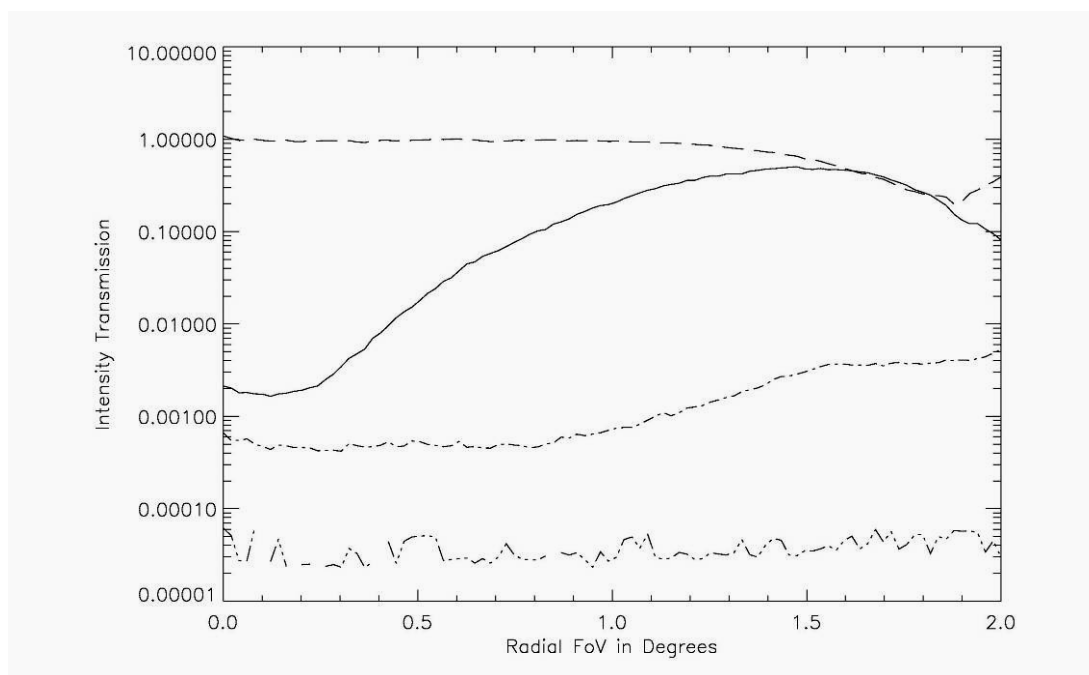


Figure 17: field dependent transmission through our Pockels cell. The solid line is the 12mm uncompensated BBO crystal. The dashed line shows the transmission when the voltage is applied to the crystal. The dashed-dotted line is the transmission in the 'closed' state of the cell. The lowest line shows the polarizers alone.

Figure 17 shows a measurement of the test cell setup. The main performances, that more than fulfills the required specifications are hereby summarized:

- Pockels cell suppression over the required  $\pm 0.8^\circ$  field of view  $< 1:5000$
- Suppression over  $\pm 4^\circ$   $1:1000$
- Transmission over  $\pm 0.8^\circ$   $> 97\%$

- No ringing present
- Risetime <10ns

## REFERENCES

- [1] Rabien, S. et al., "ARGOS - The Laser Guide Star System for the LBT", Proc. SPIE 7736-13, (2010).
- [2] Orban de Xivry G. et al. "Wide-field AO correction: the large wavefront sensor detector of ARGOS", Proc. SPIE 7736-199, (2010)
- [3] Bonaglia et al. "Diffraction limited operation with ARGOS: an hybrid AO system", Proc SPIE 7736-106, (2010)
- [4] Hart M. et al. "Diffraction-limited upgrade to ARGOS: the LBT's ground-layer adaptive optics System", Proc SPIE 7736-114, (2010)
- [5] Kanneganti S. et al. "ARGOS: a laser constellation for adaptive optics at the LBT", Proc SPIE 7736-161, (2010)
- [6] Rigaut F. "Ground conjugated adaptive optics for the ELTs", Beyond conventional adaptive optics, Proc.ESO (2001)
- [7] Esposito S. et al. "First light AO (FLAO) system for LBT: final integration and acceptance test results in Europe", SPIE 7736-12, (2010)